NASA Technical Paper 1847

Energetics of a Sudden Stratospheric Warming Simulated With a Three-Dimensional, Spectral, Quasi-Geostrophic Model

Kenneth V. Haggard and William L. Grose

MAY 1981

NASA

NASA Technical Paper 1847

Energetics of a Sudden Stratospheric Warming Simulated With a Three-Dimensional, Spectral, Quasi-Geostrophic Model

Kenneth V. Haggard and William L. Grose
Langley Research Center
Hampton, Virginia

National Aeronautics
and Space Administration

**Scientific and Technical
Information Branch**

1981

SUMMARY

This paper describes the energetics of a three-dimensional, quasi-geostrophic simulation of a sudden stratospheric warming which developed spontaneously during an annual-cycle simulation. Daily values of the stratospheric temperatures, zonal winds, heating rates, energies, and energy conversions are discussed and compared with those for observed warmings. It is shown that, like observed warmings, the simulated warming was preceded by an increased vertical flux of eddy kinetic energy from the troposphere and the polar heating resulted because of the strong convergence of the horizontal, eddy heat flux which was only partially balanced by adiabatic and diabatic cooling.

There is a significant similarity between the energetics of the simulated and observed warmings. In addition the warming was spontaneous and the model did not develop a major warming in each winter of the simulation. These facts suggest that this model may be useful for studying not only the warming process, but also the conditions that favor its development.

INTRODUCTION

Since Scherhag [1952] reported the discovery of the event now commonly referred to as a "sudden stratospheric warming," researchers have been intrigued by the occurrence of these major anomalous disturbances in the winter polar stratosphere. Individual warmings have been analyzed by various investigators during the subsequent years. Model simulations of these events also have been attempted with varying degrees of success. The monograph edited by McInturff (1978) and the reviews by Schoeberl (1978) and Quiroz et al. (1975) provide extensive discussions of both observational and model studies on this topic.

Most of the model studies of stratospheric warmings have utilized mechanistic models with prescribed boundary conditions imposed at the tropopause of the model. The studies of Matsuno (1971), Geisler (1974), Holton (1976), and Schoeberl and Strobel (1980) fall within this category. These models are of particular interest because of their apparent success in simulating a warming. However, these studies also provide some contrasting views of the dynamical evolution of a warming.

Matsuno (1971) developed a quasi-geostrophic model having a single zonal wave interacting with the mean flow. Matsuno hypothesized that planetary-scale waves propagating upward into the stratosphere would decelerate the zonal mean flow. The large amplitude of the waves at higher levels in the model, where the density is low, would be particularly effective in weakening the zonal wind and eventually producing a critical level. The critical level would then act to absorb the wave energy, producing further deceleration of the zonal flow and descent of the critical level. The Coriolis torque acting on the mean meridional circulation induced by the large convergence of the poleward, eddy heat flux was responsible for the easterly acceleration.

The studies of Geisler (1974) and Schoeberl and Strobel (1980) also utilized quasi-geostrophic models having a single zonal wave interacting with the mean flow. Schoeberl and Strobel (1980) concluded that the formation and propagation of critical levels was an essential element in the development of a warming. Geisler (1974), on the other hand, noted the formation and descent of a critical level in his study, but concluded that the warming did not result from critical-level absorption of the wave.

The results obtained by Holton (1976) provided a somewhat different explanation of the warming development. In the study with zonal wave number one, Holton found no indication of a descending critical level. He concluded that wave transience, rather than critical-level interaction, was the primary reason for the mean flow deceleration. Furthermore, he found that convergence of horizontal, eddy momentum flux was important in that it acted to approximately balance the Coriolis torque. The net deceleration of the westerlies resulted from the small residual between these two terms and was an order of magnitude smaller than the Coriolis torque.

A notable exception to the mechanistic-model studies is the simulation of stratospheric warmings with a primitive-equation, general-circulation model reported by Newson (1974) and O'Neill (1980). O'Neill noted the presence of large, equatorward, eddy momentum flux. Thus, the divergence of the horizontal momentum flux in this simulation was responsible for weakening the westerly jet. He also reported no evidence for a descending critical level and determined wave transience to be instrumental in the warming.

The present study describes the analysis of the energetics of a sudden warming which developed spontaneously during one winter of a 33-month simulation using a three-dimensional, quasi-geostrophic model. The analysis of a portion of the 33-month simulation was previously reported by Ramanathan and Grose (1978) as a study of radiative-dynamic coupling in the stratosphere. The changes that occurred in the circulation and thermal structure of the winter polar stratosphere during the warming are shown to be in close agreement with observed behavior. That is, characteristic features of stratospheric warmings reproduced by the model included: (1) enhanced vertical flux of eddy energy into the stratosphere; (2) rapid temperature increase in high latitudes with a reversal of the zonal mean temperature gradient between midlatitude and pole; (3) destruction of the circumpolar cyclonic vortex; and (4) marked deceleration of the westerly jet and the appearance of zonal mean easterlies.

It will be shown that the energetics of this simulation, as well as the dynamical development which is described by Grose and Haggard (1981), are in good agreement with features characteristic of observed warmings. It will further be shown that the present work compares well with certain aspects of other model results, but interesting contrasts are also noted. In particular, it will be shown that, like observed warmings, the simulated warming was preceded by an increased vertical flux of eddy geopotential energy from the troposphere and that polar heating resulted because of the strong convergence of the horizontal, eddy heat flux which was only partially balanced by adiabatic and diabatic cooling. A discussion of the synoptic development of this simulated warming is given by Grose and Haggard (1981).

SYMBOLS

AE	eddy available potential energy of Northern Hemisphere
AESH	eddy available potential energy of Southern Hemisphere
AF	rate of conversion of AESH to AE
AZ	zonal available potential energy of Northern Hemisphere
AZSH	zonal available potential energy of Southern Hemisphere
BAE	rate of conversion of AESH to AE by boundary flux
BAZ	rate of conversion of AZSH to AZ
BKEH	rate of conversion of KESH to KE by boundary flux
BKEV	convergence of vertical flux of KE
BKZV	convergence of vertical flux of KZ
CA	1/2(CAZ + CAE)
CAE	rate of conversion of AZSH to AE
CAZ	rate of conversion of AZ to AESH
CEA	rate of conversion of AE to KESH
CEK	rate of conversion of AESH to KE
CK	1/2(CKZ + CKE)
CKE	rate of conversion of KE to KZSH
CKZ	rate of conversion of KESH to KZ
CZA	rate of conversion of KZSH to AZ
CZK	rate of conversion of KZ to AESH
DE	dissipation of KE by friction and by diffusion
DZ	dissipation of KZ by friction and by diffusion
GE	generation of AE by diabatic heating and by diffusion
GZ	generation of AZ by diabatic heating and by diffusion
KE	eddy kinetic energy of Northern Hemisphere

KESH	eddy kinetic energy of Southern Hemisphere
KF	rate of conversion of KESH to KE
KZ	zonal kinetic energy of Northern Hemisphere
KZSH	zonal kinetic energy of Southern Hemisphere
m	order of Legendre function; zonal wave number
n	degree of Legendre function
N	north
p	pressure
$P_n^m(\mu)$	associated Legendre function of order m and degree n
Q	diabatic heating term
Q_{EX}	radiative exchange term
Q_{LW}	longwave heating term
Q_{SOL}	solar heating term
Q_{SP}	cooling to space term
t	time
VOE	vertical flux of eddy geopotential energy
VOZ	vertical flux of zonal geopotential energy
$\zeta_n^m(p,t)$	expansion coefficient; vorticity
θ	potential temperature
λ	longitude
μ	sine of latitude
ω	vertical velocity, dp/dt

Subscripts:

b	bottom of region
t	top of region

MODEL DESCRIPTION

The model used for this experiment is the one described by Ramanathan and Grose (1978) and Chen and Ramanathan (1978); hence, only a brief description of it is given here. The model is three-dimensional and quasi-geostrophic, with nine pressure levels extending from 800 to 0.05 mbar. (See fig. 1.) As shown in the figure, the potential temperature and the vertical velocity are defined at the same pressure levels, while the vorticity is defined at alternate levels. At each pressure level, the field variables are expanded in terms of spherical harmonics in the form

$$\zeta(\lambda,u,p,t) = \sum_{m=-6}^{6} \sum_{n=n_1}^{n_2} \zeta_n^m(p,t) P_n^m(u) e^{im\lambda} \qquad (1)$$

$n_1 = 1$ if $m = 0$

$= |m|$ if $m \neq 0$

$n_2 = n_1 + 5$

where λ is the longitude, u is the sine of the latitude, and $P_n^m(\mu)$ is the associated Legendre function of order m and degree n. The expansion coefficient $\zeta_n^m(p,t)$ is a function of pressure and time. The term involving P_0^0 is omitted for the temperature expansion; thus, the global mean temperature at each level is not calculated but is instead specified as the observed yearly mean of the global value for that pressure level. This expansion has six planetary waves in the longitudinal direction and provides for a three-cell latitudinal structure in each hemisphere.

This model differs from the one described by Trenberth (1973a and 1973b) by including odd orders in the spherical harmonics and in the calculation of the stratospheric diabatic heating, which is done with the model described by Ramanathan (1976). It is also similar to the model described by Cunnold et al. (1975). As in Trenberth's model, the direct effects of orography and the differential heating due to land-sea contrast are present only in zonal wave number two.

Diabatic heating in the model troposphere is calculated using the Newtonian approximation. However, for the diabatic heating Q in the stratosphere we use the method described in Ramanathan (1976) where

$$Q = Q_{SOL} + Q_{LW} \qquad (2)$$

The solar heating term Q_{SOL} includes the absorption by O_3 of the direct as well as the reflected components of the solar radiation. The longwave term Q_{LW} which includes contributions from CO_2, H_2O, and O_3 is expressed as

$$Q_{LW} = Q_{SP} + Q_{EX} \tag{3}$$

where Q_{EX} is the cooling or heating due to energy exchange between the level under consideration and the layers below, including the troposphere and the surface, and Q_{SP} is the cooling to space term. The contribution arising from energy exchange between the level and the layers above is neglected because this term has been shown to be generally negligible by Ramanathan (1976). However, Ramanathan (1977) shows that during extreme situations such as a sudden stratospheric warming, the downward, longwave radiative flux from the warm polar stratosphere to the troposphere may be of importance. The Q_{EX} term has been shown by Ramanathan and Grose (1977 and 1978) to play an important role in the stratosphere for $p > 10$ mbar. The Newtonian approximation implicitly neglects the Q_{EX} term by assuming that Q_{LW} is dependent only on the local temperature.

For the diabatic heating calculations we utilize O_3 distributions as a function of latitude, altitude, and season as tabulated by Ramanathan and Grose (1977; see their table I). For H_2O we have adopted the relative humidity distribution given by Manabe and Wetherald (1967) for the troposphere and assume a constant mass-mixing ratio of 3 parts per million by volume for the stratosphere. For CO_2, we assume a uniform distribution of 320 parts per million by volume. Doppler broadening effects for CO_2 and O_3 are included in the radiative transfer model.

DEVELOPMENT OF THE WARMING

The simulated stratospheric warming described in this paper developed spontaneously during one winter in a series of annual-cycle simulations. In contrast to model simulations such as those by Holton (1976) and Matsuno (1971), no forcing was imposed at the lower boundary nor was there any alteration of the fields that occurred naturally during the simulation. The development of a major warming was not a recurring event. Each winter simulation was marked by a series of small warmings, but major warmings developed in only two of the four winter simulations. The present analysis will be restricted to a discussion of the first of these events.

One of the most dramatic features of a major stratospheric warming is the rapid increase in the polar temperature. Histories of the zonal mean temperatures for the 40-, 10-, and 2-mbar levels are shown in figure 2. At all three levels, the histories display a series of low-amplitude oscillations at the pole throughout the first half of the winter. In mid-February, there is a pronounced warming trend at 40 mbar northward of 45° N which acts to eliminate the latitudinal temperature gradient in the higher latitudes. Similar warming occurs at both the 10- and 2-mbar levels a few days later. However, the warming at these two higher levels does not cause an initial increase in the polar temperature and, thus, temporarily acts to steepen the latitudinal temperature

gradient in the polar region. Early in March there is an increase in the 40-mbar polar temperature which peaks at 231 K on March 11 and then declines for about a week. As the 40-mbar temperature is declining, there is a rapid increase of the polar temperature at 10 mbar from 212 K on March 11 to 242 K on March 17. The decline of the 40-mbar temperature after March 11 is followed by another rapid increase to 234 K and a decline of the 10-mbar value. There is also an increase in the 2-mbar polar temperature to a peak of 242.5 K on March 21. After this, the polar temperatures at 10 and 40 mbar decline towards their more usual winter values. However, the temperature at 2 mbar does not really recover, but continues into the spring warming.

In order to be designated a major warming, not only must the zonal, mean temperature gradient reverse at or below 10 mbar but there must also be an associated circulation reversal (McIntruff 1978). The histories of the zonal winds for the 70-, 20-, and 5-mbar levels are shown in figure 3. Initially, the winds are moderate and compare well with the observations of Newell et al. (1974). However, a general strengthening of the polar-night jet at all three levels begins to occur by February 10. Centered about 30° N to 35° N, there is a region of very weak westerlies at both 70 and 20 mbar for the first half of the winter. Coincident with the first appearance of the warming trend northward of 45° N shown in figure 2, there is a deceleration of the zonal winds and the development of isolated region of easterlies centered at approximately 35° N and 20 mbar. Examination of the latitudinal structure of the wave amplitudes (see Grose and Haggard 1981) and the latitudinal distribution of the upward propagation of eddy energy from below leads us to conclude that this "critical" region does not play a role in the model warming analogous to that proposed by Matsuno (1971), where the critical level acts to absorb wave energy and to intensify the warming. In this simulation, the region appears to act as a guide for channeling large-amplitude planetary waves to higher latitudes, consistent with the results of both Matsuno (1971) and Simmons (1974). While no critical line develops at the 5-mbar level until the warming has decayed, there is a marked decrease of the zonal velocities in the midlatitudes.

With the first peak in the polar temperature at 40 mbar, the polar jet shows (fig. 3) a rapid decrease at all three levels. As the 10-mbar temperature peaks, the zonal wind almost reverses at 5 mbar, and finally, as the 40-mbar polar temperature peaks for the second time, easterlies develop at 20 mbar from approximately 45° N poleward. As the warming decays, the westerlies are reestablished, but by this time, the stratosphere is in transition to summer conditions.

HEATING RATES

In this section, the mechanisms responsible for the increases in the temperatures shown in figure 2 will be examined, and it will be shown that they are in agreement with observations. The net heating rates and the contributions due to the convergence of the horizontal, eddy heat flux, the meridional circulation, and the diabatic heating for the 40- and 10-mbar levels are shown in figure 4. Note that the meridional term is plotted with a negative sign to better show its phase relationship to, and its degree of cancellation with, the eddy convergence term. For the first half of the winter, there is, on the average, a general balance between the meridional heating and the eddy advective

heating, with a slight phase lag between the two which produces the series of low-amplitude polar warmings seen in figure 2. Starting in mid-February, there is a series of three pulses of strong, eddy heating at both levels. At the 40-mbar level, these pulses dominate the other terms and produce the increases in temperature shown in figure 2. However, at the 10-mbar level, the first pulse is effectively balanced by the meridional term and there is a net cooling during the period of the first pulse. During the rapid rise of the second pulse, there is a balance between the meridional and eddy terms, but eventually the eddy heating dominates and the net heating reaches 7 K/day. As a result, the 10-mbar polar temperature increases by 30 K in 6 days. The meridional term remains large and is, in fact, dominant during the third pulse at 10 mbar. This results in very rapid cooling. The eddy heating pulses at 10 mbar lag the corresponding 40-mbar pulses by 2 to 4 days, which suggests that the source of this heating is at lower altitudes.

Time averages of the zonal, mean heating rates as a function of latitude at the 10-mbar level are shown in figure 5. Note that the meridional term is multiplied by negative one to better show the strong degree of cancellation between it and the eddy term. The first average is for the period from December 21 to January 30 (fig. 5(a)) and illustrates conditions prior to the onset of the warming. As noted in both observational and model studies, the meridional and eddy terms tend to balance each other except near the pole. There is meridional heating in the lower latitudes between 5° and 40° N, cooling between 40° and 75° N, and heating near the pole. The second time average is for February 25 to March 3 (fig. 5(b)) and covers the time of strong, net heating near 50° N shown in figure 2(b). The peak meridional heating has moved just north of 30° N, and the maximum net heating near 50° N results largely from the eddy term. Even though the meridional and eddy terms are both large near the pole, they tend to cancel. The final average (fig. 5(c)) covers the period of March 12 to March 17 during the time of peak temperature increase at this level. The meridional heating is now a maximum near 50° N but is balanced by the eddy term, except north of 60° N. Here the eddy term dominates and is responsible for the large, polar heating northward of 60° N.

The mechanism of polar heating described here is in agreement with that found by Mahlman (1969), who showed that the convergence of the horizontal, eddy heat flux was the dominating factor in the polar region during a major stratospheric warming and that the mean flow acted to cool the region.

ENERGETICS OF THE WARMING

The energy cycle of a stratospheric warming is usually broken into two phases: the prewarming or amplification phase, and the postwarming or decay phase. Studies by Reed et al. (1963), Julian and Labitzke (1965), and Perry (1967) first demonstrated that during the first phase there is an increase of the vertical flux of eddy geopotential energy from the troposphere into the stratosphere. This increase of the vertical flux appears to be necessary for the development of a warming; however, it is not sufficient. If the stratospheric winds are favorable to vertical propagation, this tropospheric forcing can produce an increased, northward, eddy heat flux which results in strong convergence and polar heating. This eddy heating dominates the adiabatic cool-

ing, and the polar temperatures increase. After the latitudinal temperature gradient reverses, the convergence of the eddy heat flux continues to heat the polar region and there is a reversal of the normal, direct baroclinic cycle. As the warming decays, the stratosphere tends to return to its "normal" winter state, but with a much reduced barotropic conversion. This general trend will be discussed more fully in "Energetics of the Model Warming."

MODEL ENERGETICS

A block diagram illustrating the notations used for the energetics is shown in figure 6. All of the energetics terms given in this paper are for specified pressure regions and are integrated over the Northern Hemisphere. Thus, KZ is the zonal kinetic energy of the Northern Hemisphere within the specified pressure region, and AZ, AE, and KE are the corresponding notations for the zonal available potential, eddy available potential, and kinetic energies, respectively. The generation terms for the zonal and eddy available potential energies are GZ and GE; DZ and DE represent the dissipation of zonal and eddy kinetic energy. The terms VOZ and VOE represent the vertical flux of zonal and eddy geopotential energy, and the subscripts b and t refer to the flux at the bottom and top of the region, respectively. The terms AF and KF are for the redistribution of eddy energy between the hemispheres, and BAZ, BAE, and BKEH are boundary fluxes for transport from the Southern to Northern Hemisphere. The other terms, designated by the arrows between the energy modes, represent conversion rates between the energy modes. Thus both CKZ and CKE represent conversion from eddy kinetic to zonal kinetic energy, but they do not represent the same conversion. Recall that the energy in the boxes, KE and KZ in this study, are for the Northern Hemisphere; however, in a spectral model such as this where the base vectors (the spherical harmonics) are of global extent, a change in a spectral coefficient is felt globally. Because of this, there cannot be a strictly local conversion. The conversion CKE represents the conversion of Northern Hemispheric eddy kinetic energy to global zonal kinetic energy, and the conversion CKZ represents the conversion of global eddy kinetic energy to Northern Hemispheric zonal kinetic energy. Similar relationships hold for the other conversions between the energy modes. In some of the figures that follow, these two conversions have been averaged and the third letter in the symbol has been dropped. Thus

$$CK = (CKZ + CKE)/2 \tag{4}$$

and

$$CA = (CAZ + CAE)/2 \tag{5}$$

The arrows in figure 6 indicate the direction of positive flux or conversion.

ENERGETICS OF THE MODEL WARMING

There is ample evidence to suggest that the principal source of eddy energy in the lower stratosphere is the vertical flux of eddy geopotential energy from the troposphere (Dopplick 1971). Furthermore, this flux is observed to increase prior to a stratospheric warming. The history of the vertical flux of eddy geopotential energy across the 120-, 40-, and 10-mbar levels for this winter simulation is shown in figure 7. Note that negative fluxes are upwards. The most striking feature of this figure is the close correlation between the pulses of vertical flux beginnng in mid-February and the pulses of eddy heating shown in figure 4. At the 40-mbar level, the heating lags the 120-mbar flux by only 1 to 3 days. The lag is slightly longer at the 10-mbar level. This strongly suggests that the vertical flux from below provides the energy which results in the rapid polar heating in this model simulation and, thus, seems to be playing the same role found in observational studies. The magnitude of the vertical flux is in good agreement with observations. For example, Julian and Labitzke (1965) observed fluxes of -0.68 watt/m^2 for the 25-day mean prior to the 1963 warming, while Quiroz et al. (1975) observed peak fluxes of -0.6 watt/m^2 prior to the 1973 warming.

The histories of the kinetic energy for the regions from 120 to 40 mbar, 40 to 10 mbar, and 10 to 2 mbar are shown in figures 8 to 10. Each figure shows not only the zonal and eddy energies, but also the energy in each of the principal zonal wave numbers. These figures illustrate the dominance of the even zonal modes in this model. Their dominance results from having only nonzero values specified for the zonal and zonal-wave-number-two terms in the orography and in the tropospheric diabatic heating. Note that, while the odd modes are significant during the period of peak warming, they are not important in mid to late February while the warming is developing. Because of the levels at which the energies are calculated in the model, it is difficult to compare results with the various observations which are taken over different pressure and altitude bands. However, these kinetic energies compare reasonably well with the 5-year winter means given by Newell et al. (1974).

The time variations of the kinetic energy in the levels from 120 to 40 mbar (fig. 8) and 40 to 10 mbar (fig. 9) are closely correlated with the vertical flux and the polar-jet variations. The increase in the vertical flux of eddy geopotential energy is immediately followed by increases in the eddy kinetic energy. Decreases in the zonal kinetic energy, first in the 40- to 10-mbar level and then in the 120- to 40-mbar level, are a direct result of the weakening of the polar jet. In the 10- to 2-mbar level (fig. 10), the zonal kinetic energy is more evenly distributed over the hemisphere. There, the first decrease, early February, is the result of the weakening of the lower latitude winds, while the decrease in early March is related to the decrease in the higher latitude jet winds. The increases in the mode-2 energies in the lower two levels demonstrate that the vertical flux is principally in mode 2, and there was no marked increase for either level in mode 1 until the warming was well underway.

The histories of the available potential energies for the regions from 70 to 20 mbar and from 20 to 5 mbar are shown in figures 11 and 12, respectively. Again, mode 2 is the dominant eddy term in the lower level; however, there is a

more even partitioning between modes 1 and 2 at the higher level. At both levels, the onset of the warming is initially marked by decreases in the zonal, available potential energy. The response of the zonal term after the initial decrease is different in the two levels because of the different latitudinal gradient of the zonal temperature. Thus, the reversal of the gradient at the 40-mbar level results in a decrease in zonal potential energy through an increase of the polar temperatures. On the other hand, the 10-mbar temperature gradient is much larger, and while there is a local increase in AZ at the time of peak warming, it is small compared to the overall decrease in the early stages.

The principal energy conversions for this stratospheric warming are shown in figures 13 and 14. In figure 13, BKEV and BKZV are the convergences of the vertical flux of eddy and zonal kinetic energy, respectively, and CK is the average of the barotropic conversions CKE and CKZ. After an initial adjustment to winter conditions, there tends to be a balance between BKEV, CK, and BKZV. That is, the energy flow tends to be KE (troposphere) → KE (stratosphere) → KZ (stratosphere) → KZ (troposphere) in the region from 120 to 40 mbar. There are some significant variations from this cycle. As will be subsequently shown, a strong baroclinic cycle develops during the warming (after the 10th of March) and there is a sharp reduction in CK in the region from 120 to 10 mbar. The same major trend holds for the region from 70 to 10 mbar, except there is more variation in both the vertical flux convergences and CK. For the 25 days leading up to the warming, Julian and Labitzke (1965) give values of 0.680, 0.403, and -0.213 watt/m^2 for BKEV, CK, and BKZV, respectively, and the same conversions for the following 30 days were 0.347, 0.014, and -0.120 watt/m^2. The conversions shown in figure 13 agree well with their results. The kinetic energy conversions in the region from 10 to 2 mbar (fig. 13(c)) show the same general balance between BKEV, CK, and BKZV, but the period of reduced CK during and after the peak of the warming does not last more than a few days.

The baroclinic conversions CZA, CA (the average of CAZ and CAE), and CEA for the regions from 70 to 20 mbar and 20 to 5 mbar are shown in figure 14. This model does not produce an AE to KE conversion in the lower stratosphere, as was observed by Dopplick (1971). Instead, the winter cycle bears more resemblance to his March values in that there is a definite KE to AE conversion below 5 mbar with a strong convergence of the vertical, eddy flux throughout the winter. The available potential energy conversions are characterized by rapid variations with a period of about 1 week during the first part of the winter. For the region from 70 to 20 mbar, an indirect baroclinic cycle develops from the first of March until the midlatitude-to-pole temperature gradient returns to its prewarming state. Prior to March 1, no direct cycle was established in that both the magnitudes and direction of the conversion varied. In contrast, there was a direct, steady baroclinic cycle established in the region from 20 to 5 mbar between the latter part of February and the time that the midlatitude-to-pole temperature gradient reversed. An indirect cycle was then established and maintained until the latitudinal temperature gradient recovered to its normal winter state. This is in agreement with observations such as that by Reed et al. (1963) which analyzed the 1957 warming and showed a reversal from a direct to an indirect baroclinic cycle corresponding to the amplification and decay of the warming, respectively.

CONCLUDING REMARKS

A spontaneously produced simulation of a major, sudden stratospheric warming has been analyzed. The onset of the warming was marked by a rapid increase in the vertical flux of eddy energy out of the troposphere that was typical of observed prewarming conditions. The polar heating resulted from increased convergence of the horizontal, eddy heat flux, again as observed in actual warmings. There was no evidence of the development and subsequent descent of a horizontal critical level as postulated by Matsuno (J. Atmos. Sci., Nov. 1971). The general characteristics of the energy cycle closely resemble observations, in that the model develops a definite indirect baroclinic cycle and there is a sharp reduction of the barotropic conversion with the reversal of the midlatitude-to-pole temperature gradient in the stratosphere.

The facts that this simulation developed spontaneously, a warming does not develop each winter, and so many features of the model warming are similar to observed features, suggest that this model may be useful for studying not only the warming process but also the conditions that favor its development.

Langley Research Center
National Aeronautics and Space Administration
Hampton, VA 23665
April 6, 1981

REFERENCES

Chen, Tsing-Chang; and Ramanathan, V. 1978: A Numerical Simulation of Seasonal Stratospheric Climate: Part II. Energetics. J. Atmos. Sci., vol. 35, no. 4, pp. 615-633.

Cunnold, D.; Alyea, F.; Phillips, N.; and Prinn, R. 1975: A Three-Dimensional Dynamical-Chemical Model of Atmospheric Ozone. J. Atmos. Sci., vol. 32, no. 1, pp. 170-194.

Dopplick, T. G. 1971: The Energetics of the Lower Stratosphere Including Radiative Effects. Q. J. R. Meteorol. Soc., vol. 97, no. 412, pp. 209-237.

Geisler, J. E. 1974: A Numerical Model of the Sudden Stratospheric Warming Mechanism. J. Geophys. Res., vol. 79, no. 33, pp. 4989-4999.

Grose, William L.; and Haggard, Kenneth V. 1981: Numerical Simulation of a Sudden Stratospheric Warming With a 3-D Spectral Quasi-Geostrophic Model. J. Atmos. Sci., vol. 38, no. 7 (To be published).

Holton, James R. 1976: A Semi-Spectral Numerical Model for Wave-Mean Flow Interactions in the Stratosphere: Application to Sudden Stratospheric Warmings. J. Atmos. Sci., vol. 33, no. 8, pp. 1639-1649.

Julian, Paul R.; and Labitzke, Karin B. 1965: A Study of Atmospheric Energetics During the January-February 1963 Stratospheric Warming. J. Atmos. Sci., vol. 22, no. 6, pp. 597-610.

Mahlman, J. D. 1969: Heat Balance and Mean Meridional Circulations in the Polar Stratosphere During the Sudden Warming of January 1958. Mon. Weather Rev., vol. 97, no. 8, pp. 534-540.

Manabe, Syukuro; and Wetherald, Richard T. 1967: Thermal Equilibrium of the Atmosphere With a Given Distribution of Relative Humidity. J. Atmos. Sci., vol. 24, no. 3, pp. 241-259.

Matsuno, Taroh 1971: A Dynamical Model of the Stratospheric Sudden Warming. J. Atmos. Sci., vol. 28, no. 8, pp. 1479-1494.

McInturff, Raymond M., ed. 1978: Stratospheric Warmings: Synoptic, Dynamic and General-Circulation Aspects. NASA RP-1017.

Newell, Reginald E.; Herman, Gerald F.; Fullmer, James W.; Tahnk, William R.; and Tanaka, Minoru 1974: Diagnostic Studies of the General Circulation of the Stratosphere. Proceedings of the International Conference on Structure, Composition and General Circulation of the Upper and Lower Atmospheres and Possible Anthropogenic Perturbations, Volume I, Int. Assoc. Meteorol. & Atmos. Phys., pp. 17-82.

Newson, R. L. 1974: An Experiment With a Tropospheric and Stratospheric Three-Dimensional General-Circulation Model. Proceedings of the Third Conference on the Climatic Impact Assessment Program, Anthony J. Broderick and Thomas M. Hard, eds., DOT-TSC-OST-74-15, U.S. Dep. Transp., pp. 461-474. (Available from DTIC as AD A003 846.)

O'Neill, A. 1980: The Dynamics of Stratospheric Warmings Generated by a General Circulation Model of the Troposphere and Stratosphere. Q. J. R. Meteorol. Soc., vol. 106, no. 450, pp. 659-690.

Perry, John S. 1967: Long-Wave Energy Processes in the 1963 Sudden Stratospheric Warming. J. Atmos. Sci., vol. 24, no. 5, pp. 539-550.

Quiroz, R. S.; Miller, A. J.; and Nagatani, R. M. 1975: A Comparison of Observed and Simulated Properties of Sudden Stratospheric Warmings. J. Atmos. Sci., vol. 32, no. 9, pp. 1723-1736.

Ramanathan, V. 1976: Radiative Transfer Within the Earth's Troposphere and Stratosphere: A Simplified Radiative-Convective Model. J. Atmos. Sci., vol. 33, no. 7, pp. 1330-1346.

Ramanathan, V. 1977: Troposphere-Stratosphere Feedback Mechanism: Stratospheric Warming and Its Effect on the Polar Energy Budget and the Tropospheric Circulation. J. Atmos. Sci., vol. 34, no. 3, pp. 439-447.

Ramanathan, V.; and Grose, W. L. 1977: A Three-D Circulation Model Study of the Radiative-Dynamic Coupling Within the Stratosphere. Beitr. Phys. Atmos., vol. 50, no. 1-2, pp. 55-70.

Ramanathan, V.; and Grose W. L. 1978: A Numerical Simulation of Seasonal Stratospheric Climate: Part I. Zonal Temperatures and Winds. J. Atmos. Sci., vol. 35, no. 4, pp. 600-614.

Reed, Richard J.; Wolfe, John L.; and Nishimoto, Hiroshi 1963: A Spectral Analysis of the Energetics of the Stratospheric Sudden Warming of Early 1957. J. Atmos. Sci., vol. 20, no. 4, pp. 256-275.

Scherhag, R. [1952]: Die Explosionsartigen Stratospharenerwarmungen des Spatwinters 1951-52 (The Explosive-Type Stratospheric Warming of Late Winter, 1951-52). Ber. Deut. Wetterd., vol. 6, pp. 51-63.

Schoeberl, Mark R. 1978: Stratospheric Warmings: Observations and Theory. Rev. Geophys. & Space Phys., vol. 16, no. 4, pp. 521-538.

Schoeberl, Mark R.; and Strobel, Darrell F. 1980: Numerical Simulation of Sudden Stratospheric Warmings. J. Atmos. Sci., vol. 37, no. 1, pp. 214-236.

Simmons, A. J. 1974: Baroclinic Instability at the Winter Stratopause. Q. J. R. Meteorol. Soc., vol. 100, no. 426, pp. 531-540.

Trenberth, Kevin E. 1973(a): Global Model of the General Circulation of the Atmosphere Below 75 Kilometers With an Annual Heating Cycle. Mon. Weather Rev., vol. 101, no. 4, pp. 287-305.

Trenberth, Kevin E. 1973(b): Dynamic Coupling of the Stratosphere With the Troposphere and Sudden Stratospheric Warmings. Mon. Weather Rev., vol. 101, no. 4, pp. 306-322.

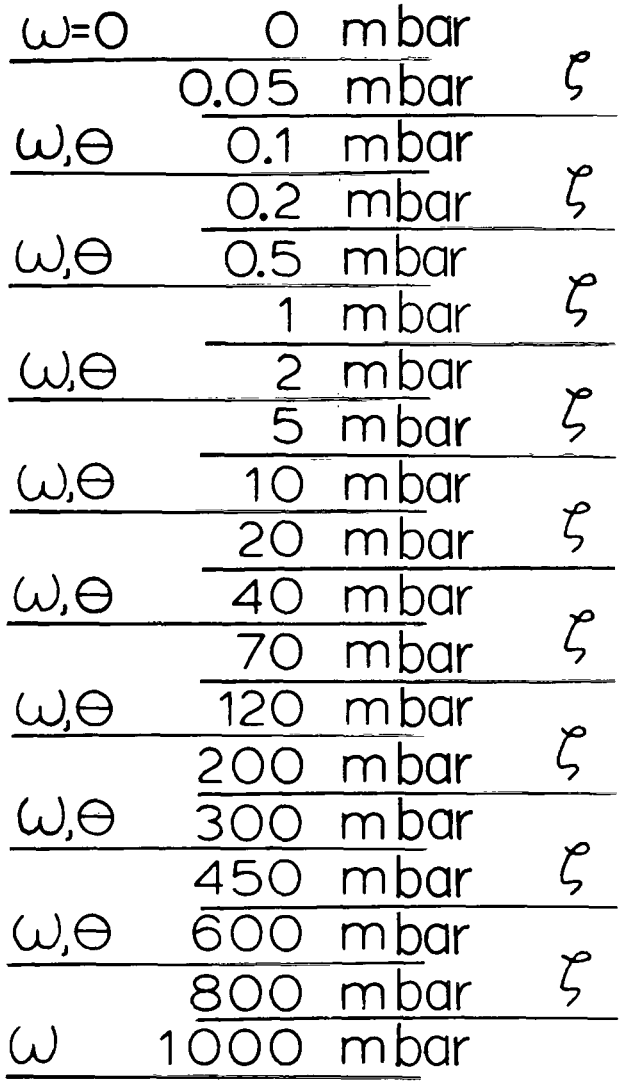

Figure 1.- Vertical resolution for model (ζ is vorticity, θ potential temperature, and $\omega = dp/dt$).

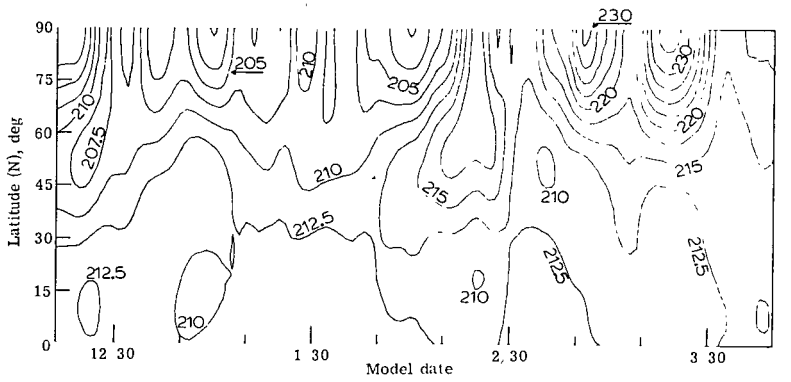

(a) 40 mbar.

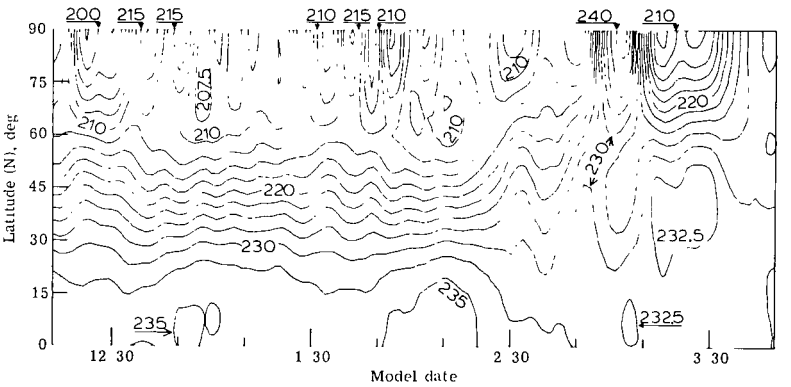

(b) 10 mbar.

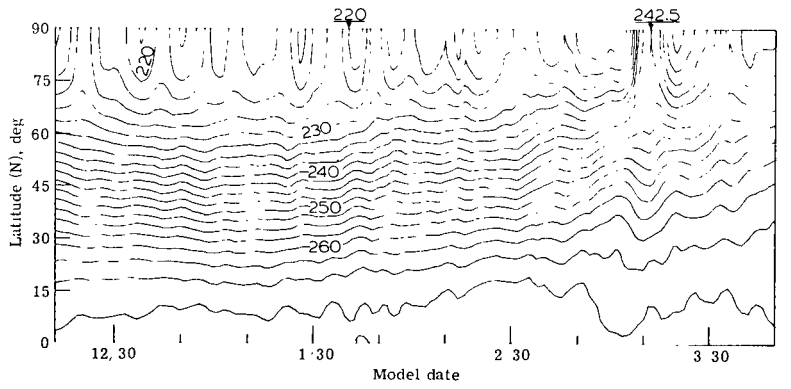

(c) 2 mbar.

Figure 2.- Zonal temperature (K) as function of latitude and time.

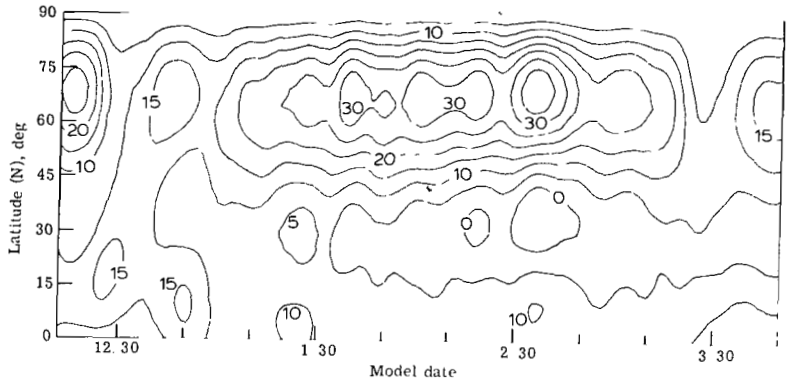

(a) 70 mbar.

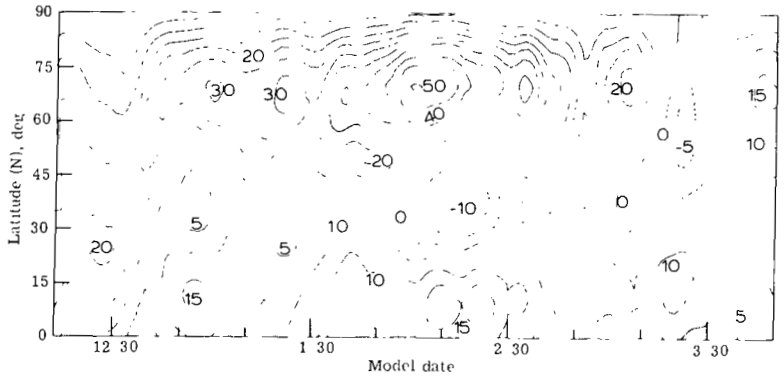

(b) 20 mbar.

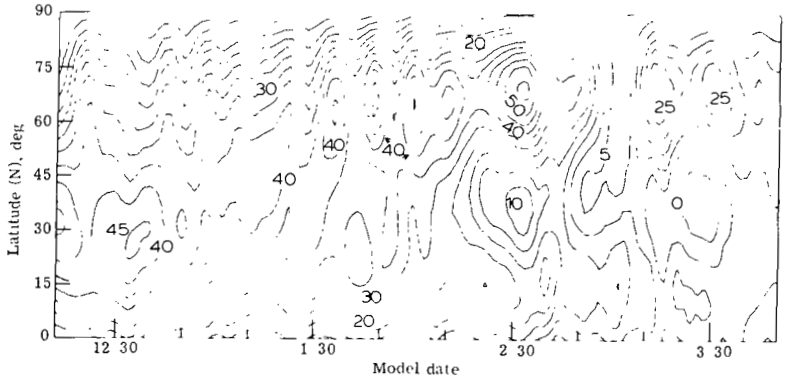

(c) 5 mbar.

Figure 3.- Zonal wind (m/s) as function of latitude and time; positive westerly.

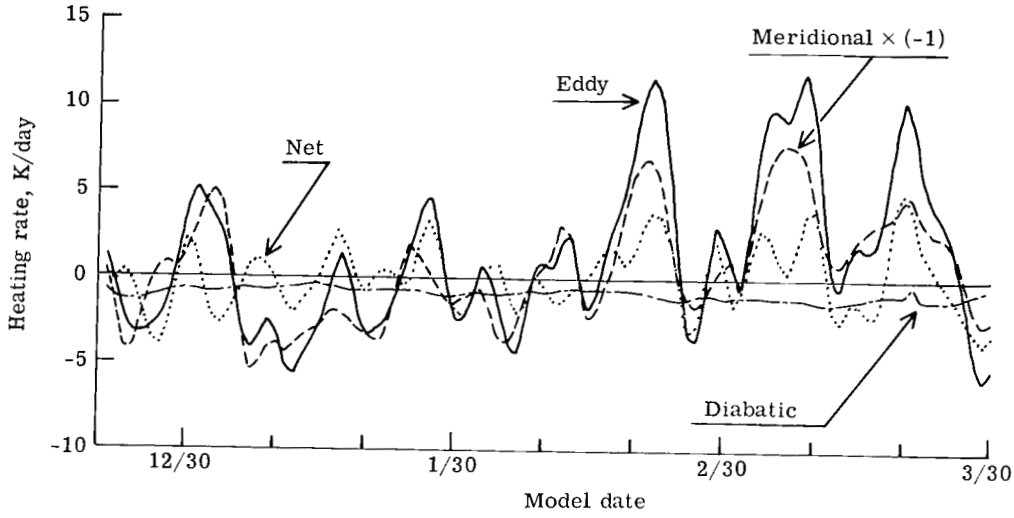

(a) 40 mbar.

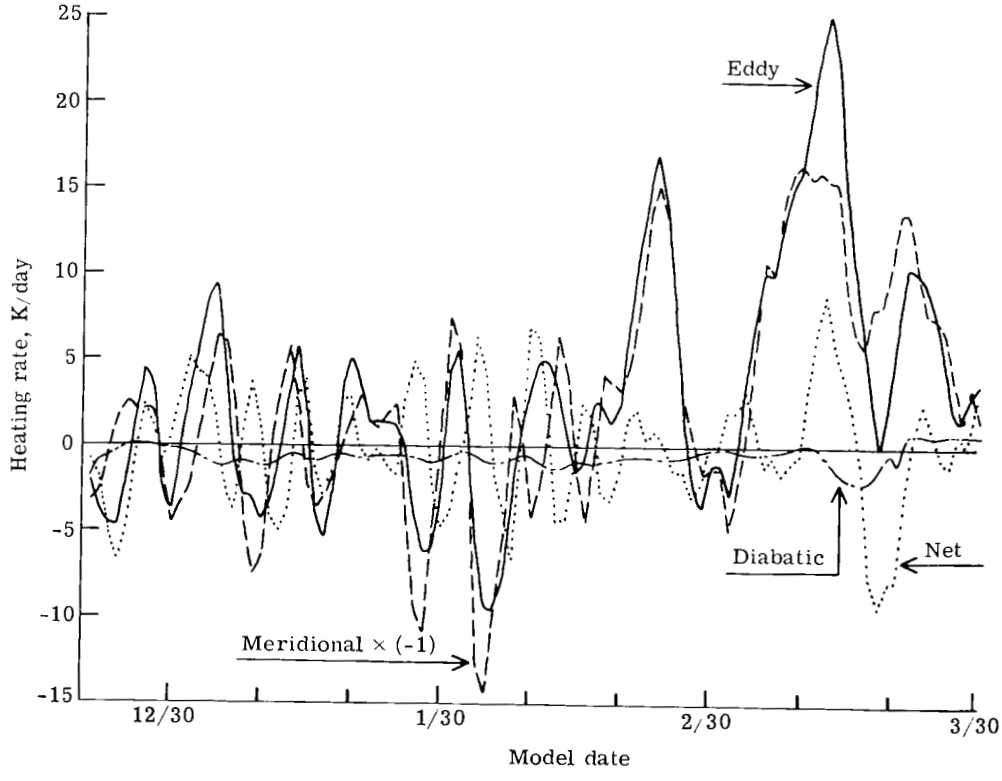

(b) 10 mbar.

Figure 4.- Heating rates at 90° N as function of time.

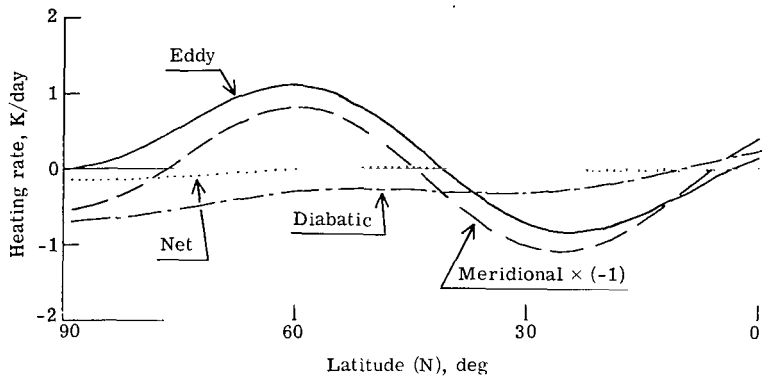

(a) 12/21 to 1/30.

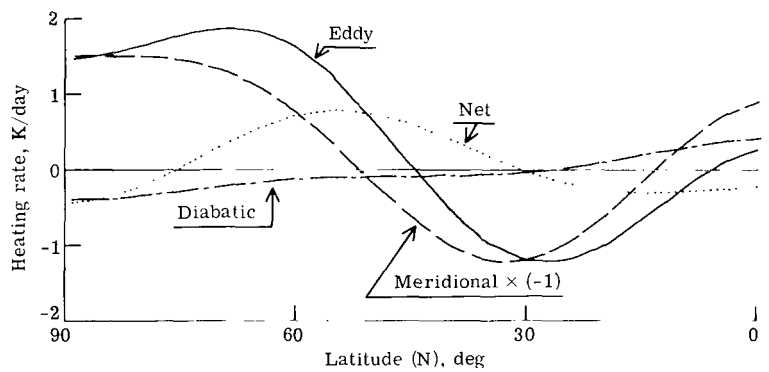

(b) 2/25 to 3/3.

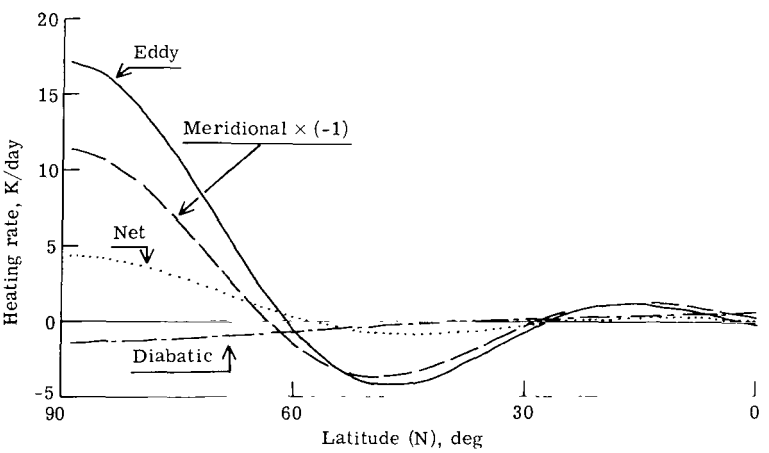

(c) 3/12 to 3/17.

Figure 5.- Zonal heating rates at 10 mbar.

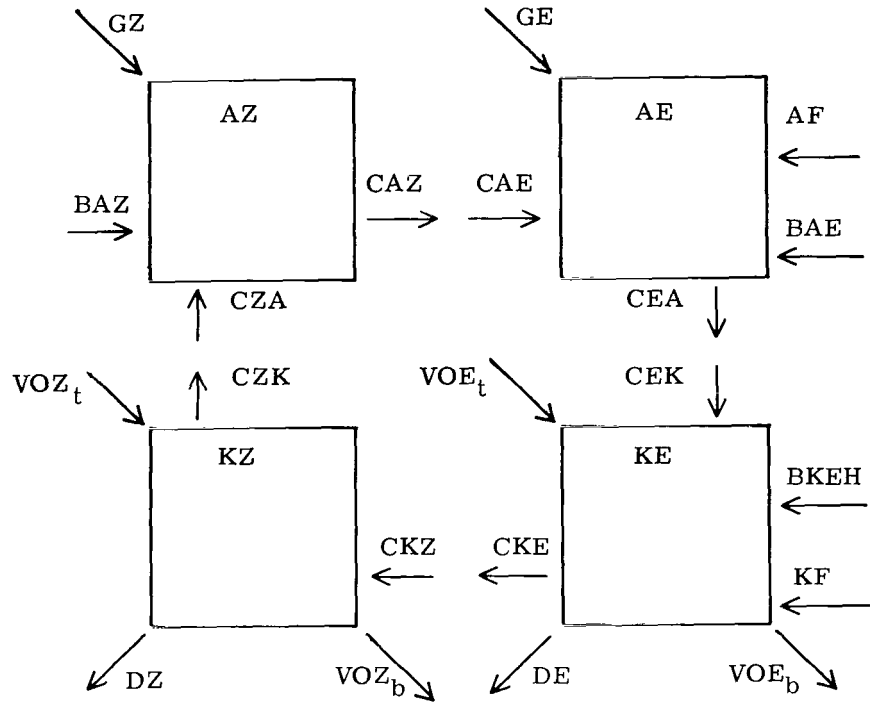

Figure 6.- Block diagram of notations for energies and energy conversions.

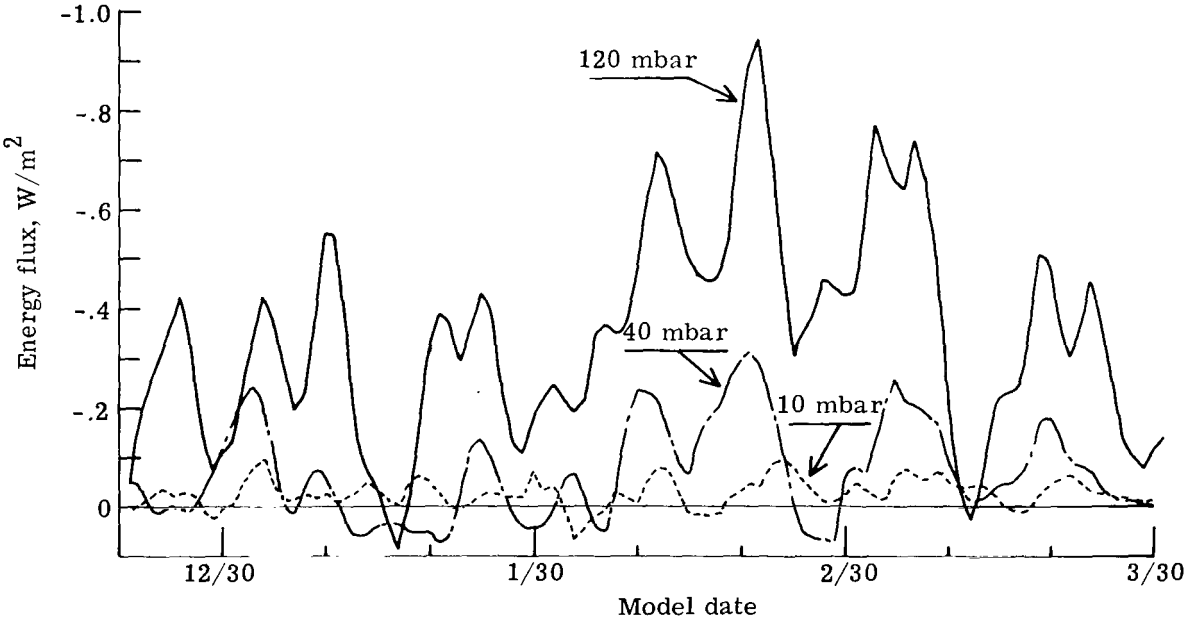

Figure 7.- Vertical flux of eddy geopotential energy as function of time.

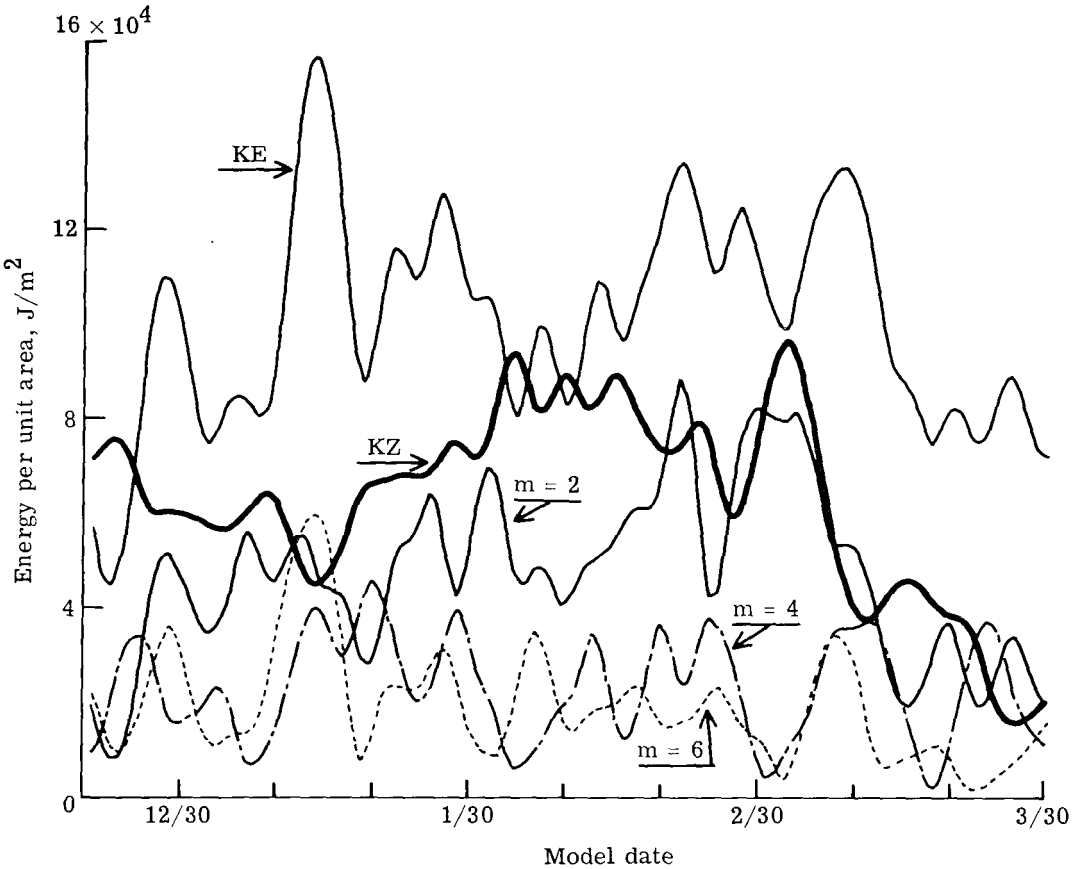

(a) Total and even zonal wave numbers.

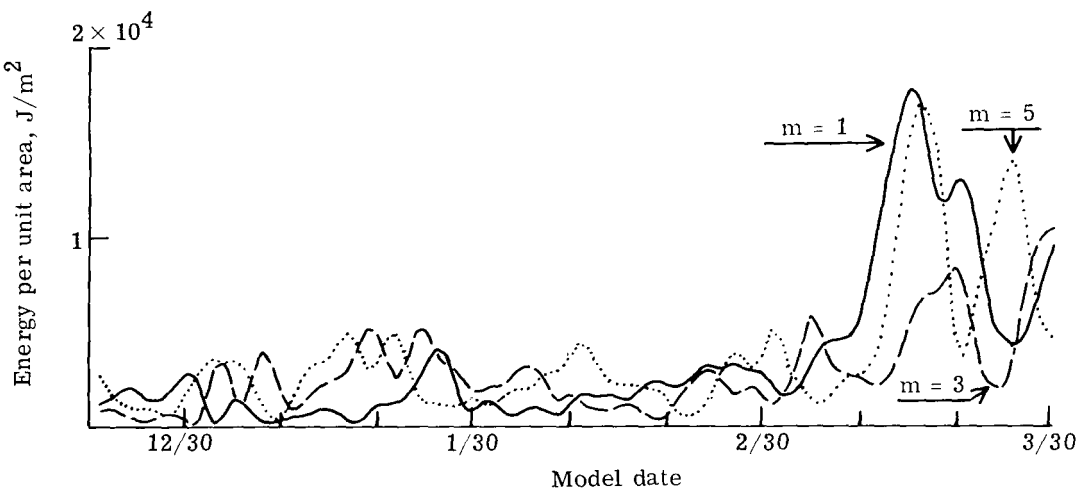

(b) Odd zonal wave numbers.

Figure 8.- Kinetic energy as function of time for Northern Hemisphere between 120 and 40 mbar.

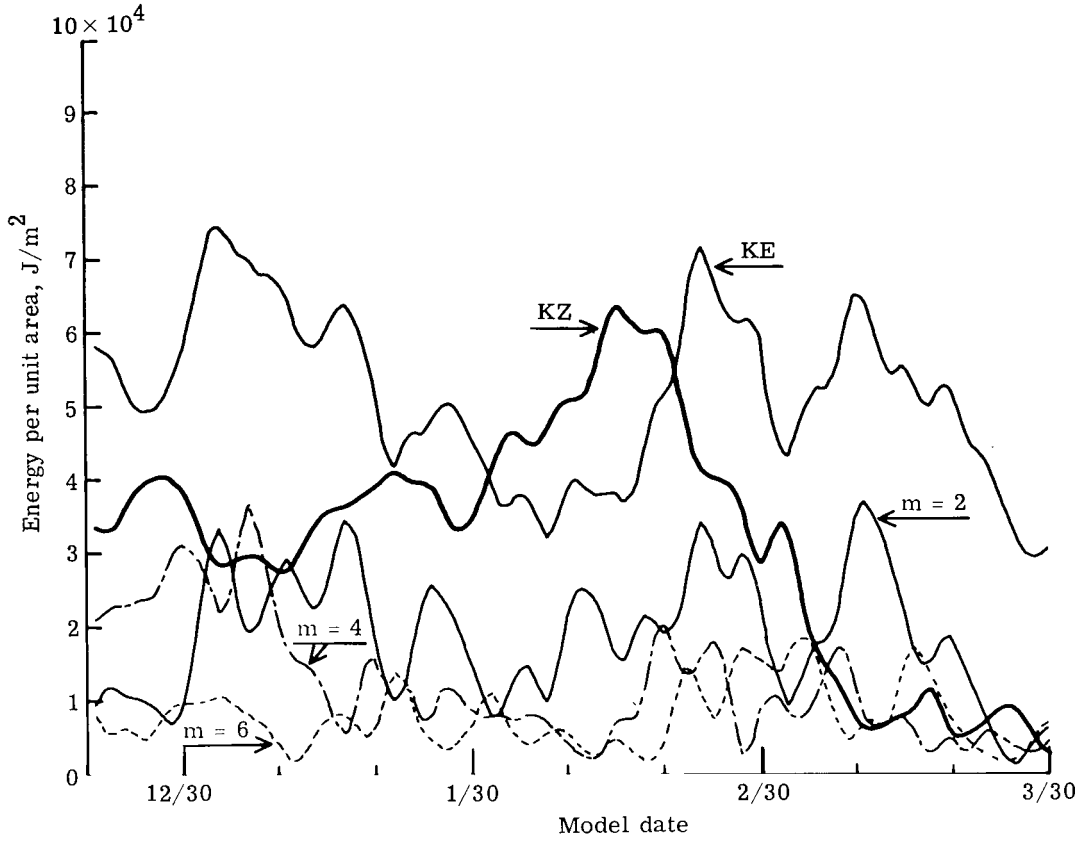

(a) Total and even zonal wave numbers.

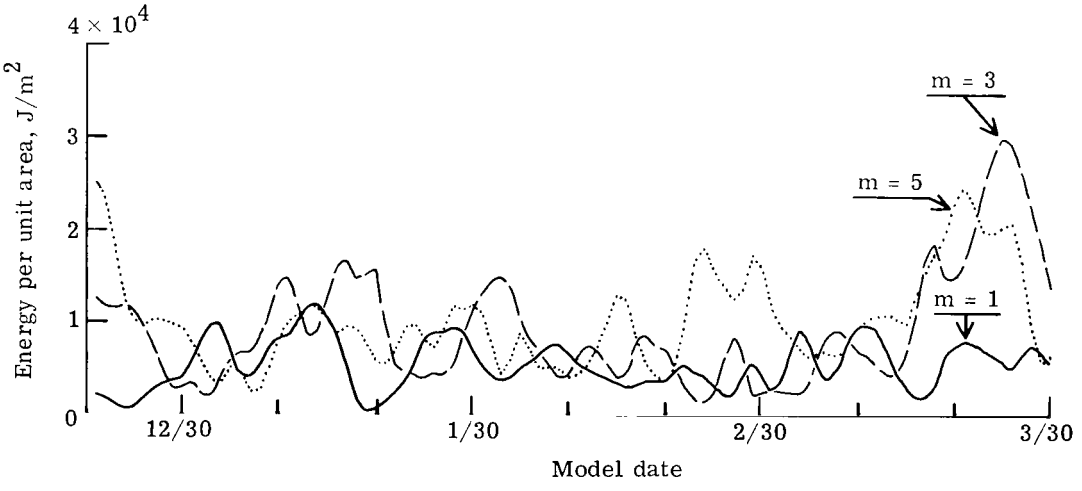

(b) Odd zonal wave numbers.

Figure 9.- Kinetic energy as function of time for Northern Hemisphere between 40 and 10 mbar.

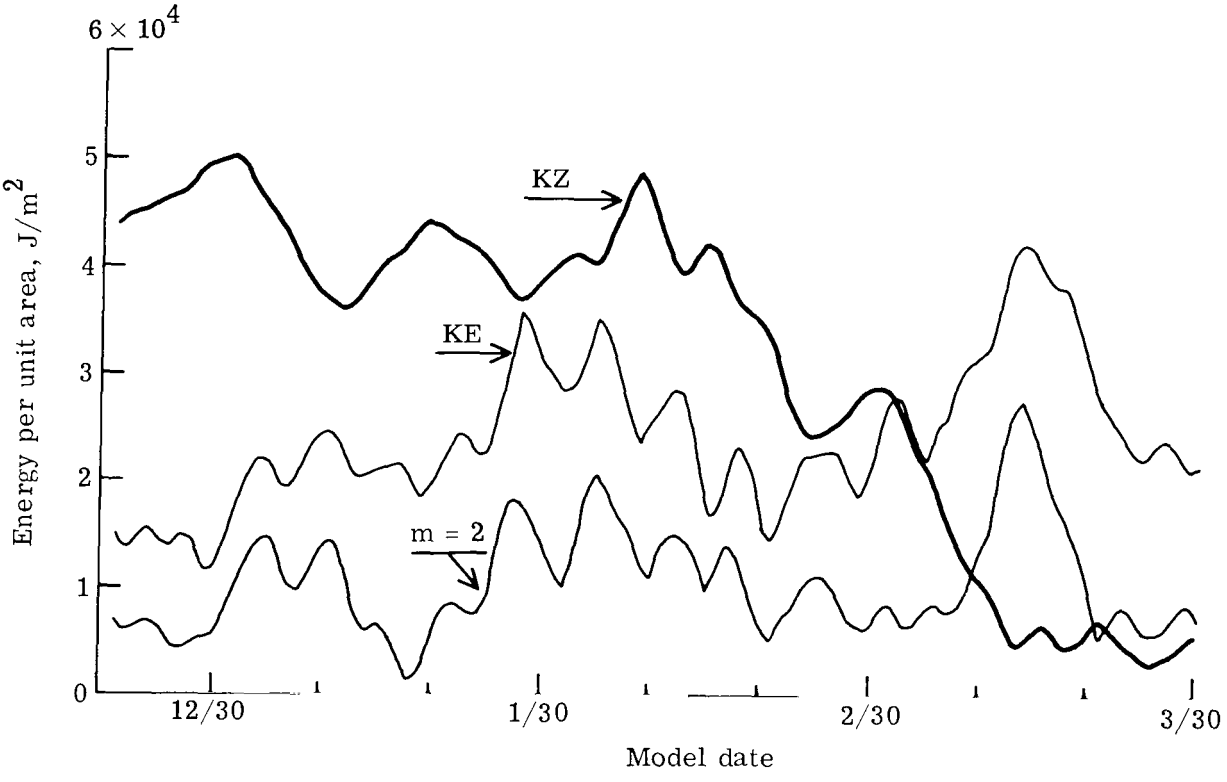

Figure 10.- Kinetic energy as function of time for Northern Hemisphere between 10 and 2 mbar.

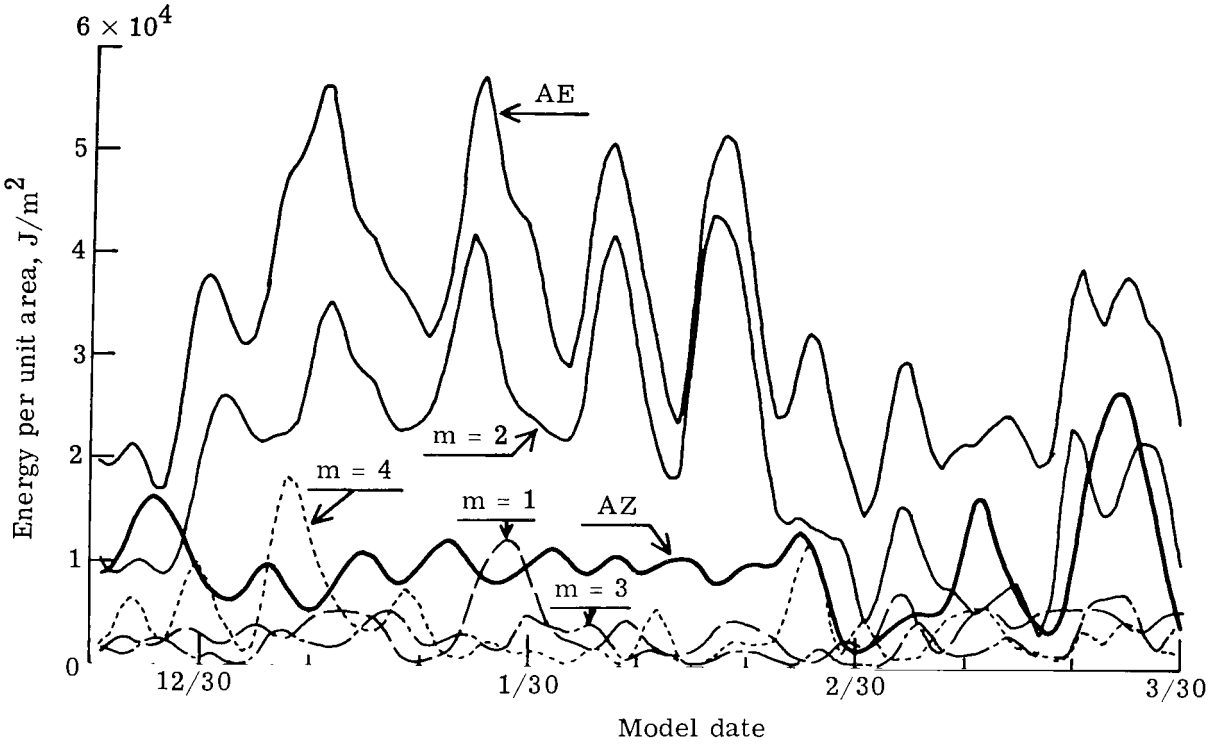

Figure 11.- Available potential energy as function of time for Northern Hemisphere between 70 and 20 mbar.

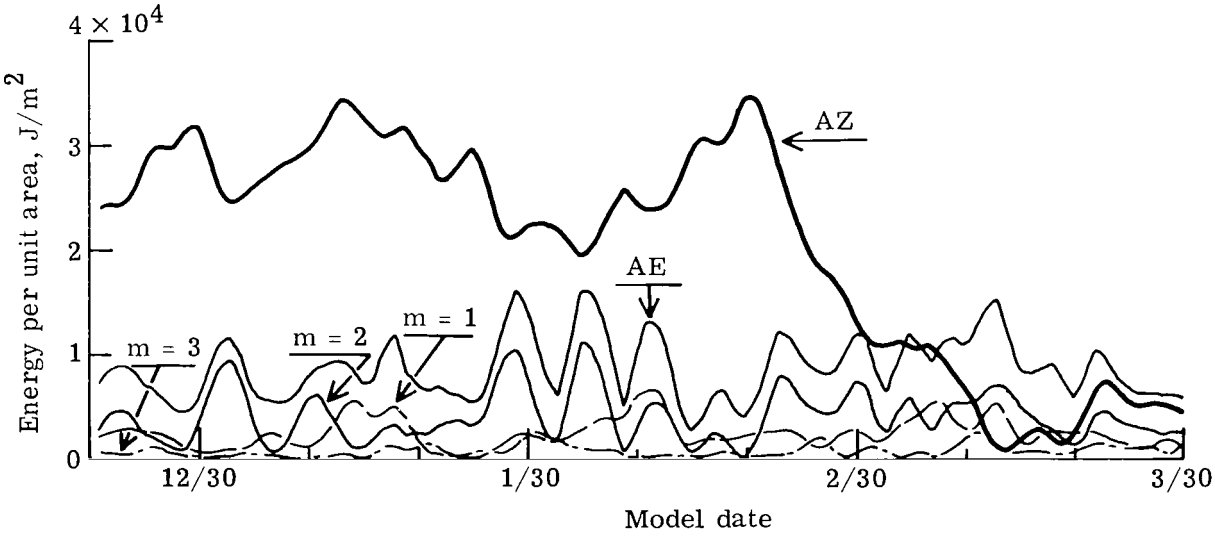

Figure 12.- Available potential energy as function of time for Northern Hemisphere between 20 and 5 mbar.

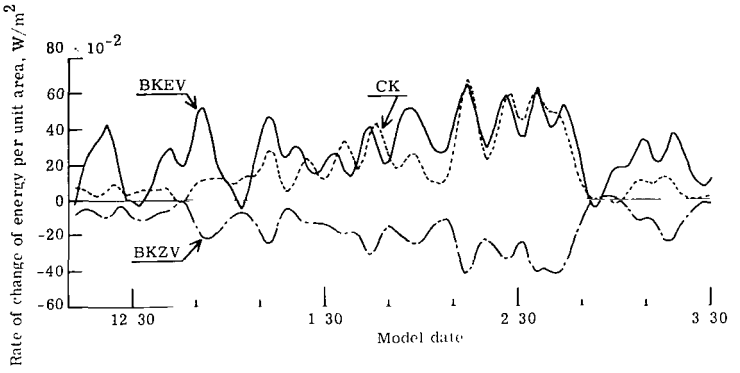

(a) 120 to 40 mbar.

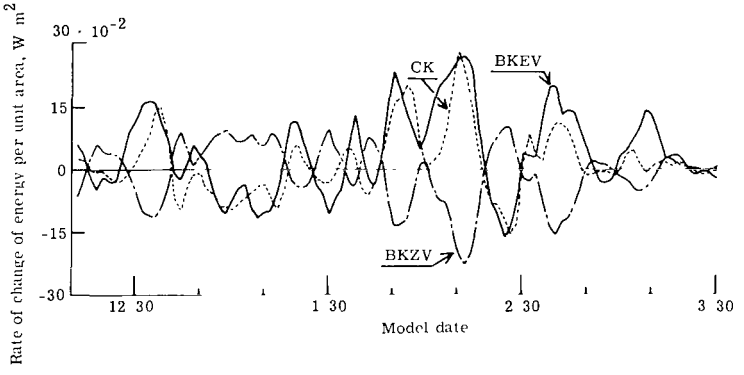

(b) 40 to 10 mbar.

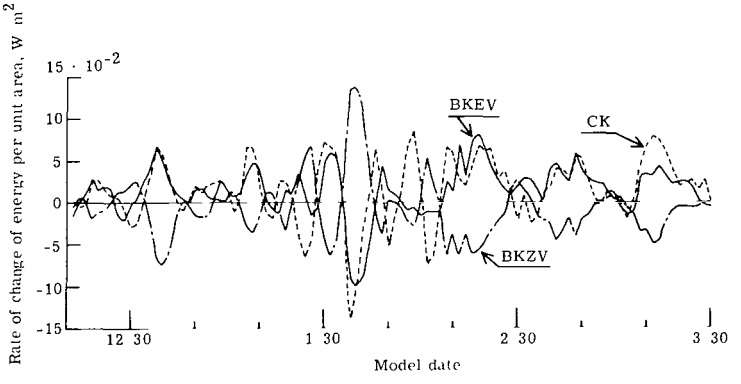

(c) 10 to 2 mbar.

Figure 13.- Kinetic energy conversions as function of time for Northern Hemisphere.

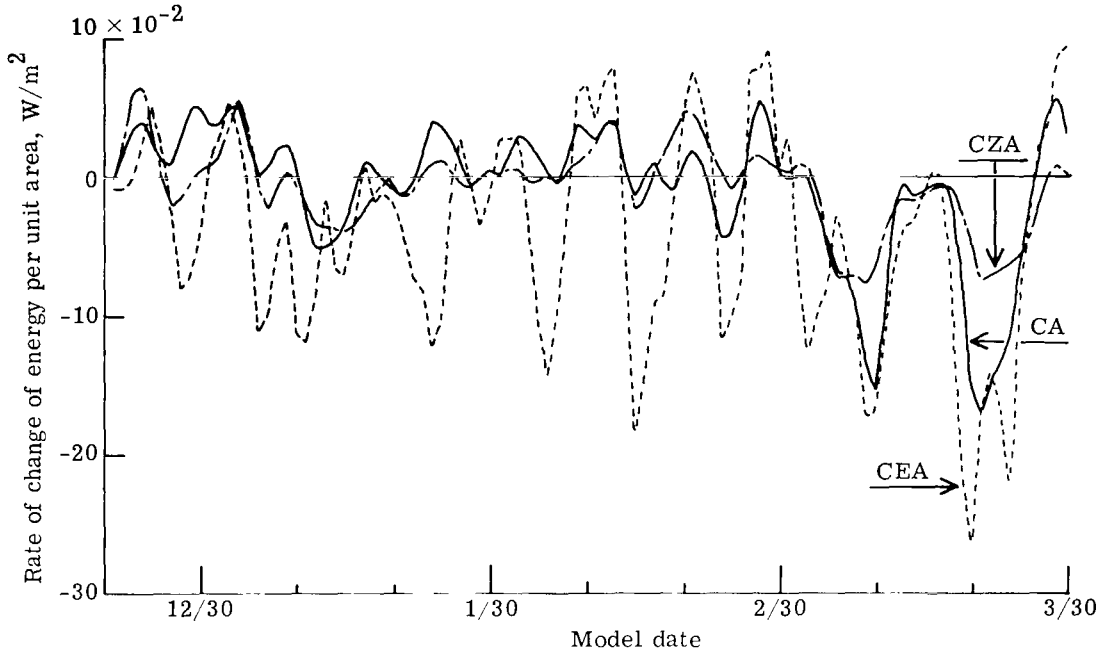

(a) 70 to 20 mbar.

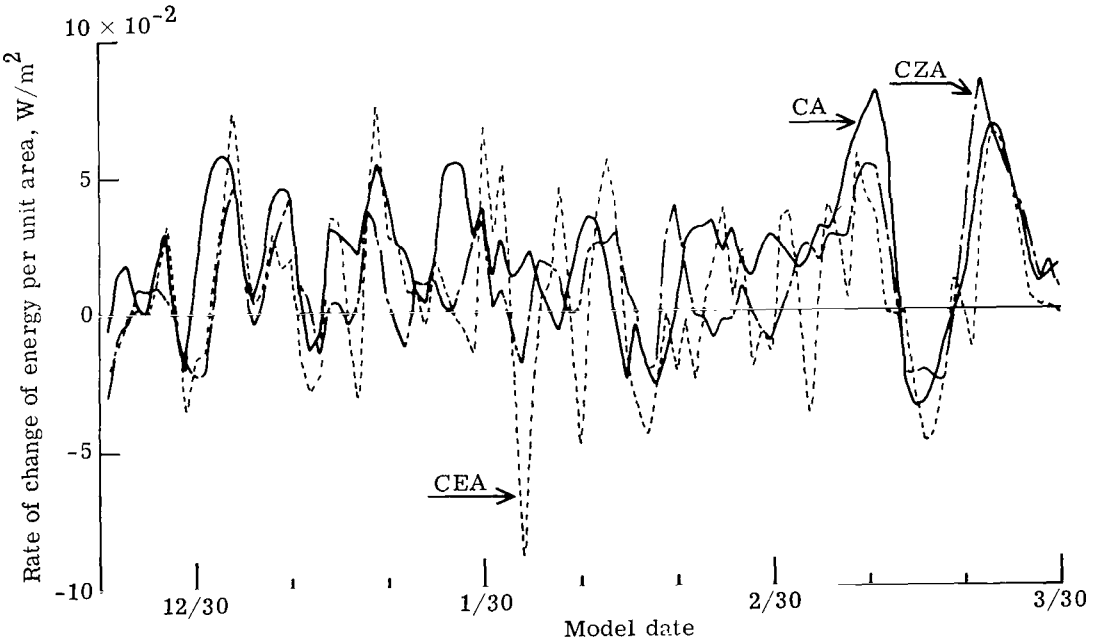

(b) 20 to 5 mbar.

Figure 14.- Available potential energy conversions as function of time for Northern Hemisphere.

1. Report No.	2. Government Accession No.	3. Recipient's Catalog No.
NASA TP-1847		

4. Title and Subtitle	5. Report Date
ENERGETICS OF A SUDDEN STRATOSPHERIC WARMING SIMULATED WITH A THREE-DIMENSIONAL, SPECTRAL, QUASI-GEOSTROPHIC MODEL	May 1981
	6. Performing Organization Code 146-60-01-06

7. Author(s)	8. Performing Organization Report No.
Kenneth V. Haggard and William L. Grose	L-14245
	10. Work Unit No.

9. Performing Organization Name and Address	11. Contract or Grant No.
NASA Langley Research Center Hampton, VA 23665	
	13. Type of Report and Period Covered Technical Paper

12. Sponsoring Agency Name and Address	14. Sponsoring Agency Code
National Aeronautics and Space Administration Washington, DC 20546	

15. Supplementary Notes

16. Abstract

This paper describes the energetics of a three-dimensional, quasi-geostrophic simulation of a sudden stratospheric warming which developed spontaneously during an annual-cycle simulation. Daily values of the stratospheric temperatures, zonal winds, heating rates, energies, and energy conversions are discussed and compared with those for observed warmings. It is shown that, like observed warmings, the simulated warming was preceded by an increased vertical flux of eddy kinetic energy from the troposphere and the polar heating resulted because of the strong convergence of the horizontal, eddy heat flux which was only partially balanced by adiabatic and diabatic cooling. There is a significant similarity between the energetics of the simulated and observed warmings. In addition, the warming was spontaneous and the model did not develop a major warming in each winter of the simulation. These facts suggest that this model may be useful for studying not only the warming process but also the conditions that favor its development.

17. Key Words (Suggested by Author(s))	18. Distribution Statement
Stratospheric warming Stratospheric energetics Global circulation model	Unclassified - Unlimited Subject Category 47

19. Security Classif. (of this report)	20. Security Classif. (of this page)	21. No. of Pages	22. Price
Unclassified	Unclassified	27	A03

For sale by the National Technical Information Service, Springfield, Virginia 22161

NASA-Langley, 1981

10 1 1U,E, 050681 S00903DS
DEPT OF THE AIR FORCE
AF WEAPONS LABORATORY
ATTN: TECHNICAL LIBRARY (SUL)
KIRTLAND AFB NM 87117